

Insulating Biomaterials N01-NS-9-2323

Fourth Quarterly Progress Report July-September, 2000

National Institutes of Health

National Institute of Neurological Disorders and Stroke

Neural Prosthesis Program

by



rSea Technology

Contributors:

David J. Edell, PI

Lydia Y. Li, Surgery and Testing

Ying Ping Liu, Assembly and Testing

Sean Sexton, Instrumentation and Software

Karen K. Gleason, Chem Eng (MIT)

Thomas B. Casserly, Grad Student, Chem Eng (MIT-HFCVD Silicones)

Shashi K. Murthy, Grad Student, Chem Eng (MIT-CVD Fluoro-silicones)



Instrumentation for In-Vitro Monitoring of Long Term Devices

Sporadic System Errors: Data from the 384 channel electrometer system has been difficult to interpret in the last attempt at a detailed review. Apparently there is an intermittent software or hardware error that is corrupting data. A thorough examination of the system was undertaken to determine the problems. Two problems were identified and have been corrected. Neither problem showed up in the calibration procedure used. The calibration procedure previously used consisted of operating one box at a time with calibration resistor arrays plugged into the test ports of the box. One problem with the calibration procedure was that the resistors used were generally very close to each other in value which made it difficult to detect faulty multiplexer switching as long as one channel was switched in during the calibration check. A second problem was that only one test box was active during most of the calibration procedures used. This wasn't viewed as a risky situation at the time because the boxes operated independently.

Two problems with the system were identified. The first of these problems was that the system seemed to switch channels spontaneously. We found two problems associated with this type of malfunction. One was that a multiplexer on the Data Translation 727 board had failed. The output showed an incorrect value for 8 of the multiplexed inputs. The problem was traced to a malfunctioning multiplexer chip on the board. The board was repaired, and an additional board was purchased to speed the reconstruction of the system. This problem affected 4 devices in box 2.

The second problem was much more ominous. The 727 multiplexer board has a set of jumpers which when installed allow the data acquisition board to read back the configuration of the board (single ended/differential, etc.). The data lines used to set the channel are the same ones used to read back the configuration data. This is done using a resistor, which is set as a pull up with the programming jumper. The idea being that the data acquisition board will have enough drive to overcome the resistor, when setting the channel. Unfortunately, our method of



connecting the 727's through our distribution board (which allows us additional channels as mentioned above) did not take this resistor arrangement into account. Thus there were 6 of these pull up resistors connected in parallel, creating an excessive load on the data acquisition board causing it to fail sporadically. This error had the potential of corrupting the data of any channel, at any time. The problem would have first appeared after the final set of 2 boxes were completed and brought on line, since fewer than 5 resistors in parallel was insufficient to load the drivers to the point of failure. The remedy for this problem was the removal of all of the configuration read-back jumpers, since we don't use this feature.

Exhaustive testing of the switching of all multiplexers was then performed, and a switching monitor has been left in place to allow casual observation of the switching to guard against future problems.

Alteration of 384 Channel System to add Dual Range Function: Because we now have so many samples under test, it has become impossible to locate samples at appropriate temperatures at a particular sensitivity. The original design did not allow for changing the range of the electrometers because it was viewed as too expensive and time consuming to implement and it was felt that simply changing the range of some of the electrometer boxes would be sufficient. However, we now have many samples that require either a high or low range for proper testing. Low range samples which provide larger currents to be measured include polyimide samples, many plasma deposited materials, and large area triple track and large area surface properties testers. The original system is described below, followed by a description of the modifications.

The soak test system consists of 6 equipment enclosures, each containing 16 custom 4-channel electrometer cards, a custom interconnection board, and a Data Translation DT727 64 channel multiplexer. In addition, a Pentium class computer contains a Data Translation DT31EZ data acquisition card, which offers 16 analog inputs, 2 analog outputs, and 16 digital IO lines. Two Hewlett Packard



power supplies provide the needed +/- 15 volts for powering the system. A custom program written in HPVee, in concert with Data Translation DTVPI interface software, handles the data acquisition. Devices are connected to the system via 25 pin dsub connectors. The devices are continually under bias.

The 4 channel electrometer cards use Analog Devices' AD549JH monolithic electrometer operational amplifier as the input amplifier. Each amplifier is connected in a current to voltage configuration with a high value (10,000 M Ω typical) feedback resistor, and a low leakage feedback capacitor to remove, from the data, the water droplet artifact caused by condensation. The output of this initial stage is then buffered through an inverting amplifier (OP-27) with a gain of either unity or 100 depending on the box. The bias voltage is fed through 10K resistors to prevent the bias voltage from being loaded down by shorted DUT's. The output of this board is connected to our custom interconnect panel which routes power, switching signals, bias voltages, and electrometer outputs to there respective locations. Each interconnect board is jumpered specifically for the box number it is in, so there is no confusion in the system of data acquisition..

The system uses the DT727 multiplexers to sequence the data onto one of 6 analog inputs to the DT31EZ (one input per box). Normally the DT727 is limited to a maximum of 256 channels (4 units daisy chained), but our custom interconnection board allows for more. In theory the number of available analog inputs of the data acquisition card sets the limit of DT727's to 16 per acquisition card. However, we are limited to 6 by the need to monitor other parameters. We set the bias on the devices using the analog output of the DT31EZ, buffer this voltage in each box, and read back the bias level after the buffer, to insure the voltage is actually present. We also monitor ambient temperature and humidity using two more inputs to the DT31EZ.

The 96 channel electrometer boxes are paired with each of three device holders set to one of three temperature levels (37°C, 80°C, and 90°C). The higher temperature boxes have their devices mounted in sealed tubes, set in a block heater. The low temperature devices are placed in short sealed jars and set in an



incubator. Temperature is regulated using custom built controllers, based on Omega Engineering's CN6700 series control.

The system uses a minimum amount of hardware. The data acquisition computer is currently a Pentium II 300Mhz CPU w/128Mb ram, and a 6Gb disk. The device test consists of stepping the voltage bias on the device, and measuring the leakage current at that bias. A full sweep consists of 23 voltage steps. Once the bias is set on a device, we wait for 10 time constants for settling before measuring the leakage.

Modification Details: In a major system upgrade begun in the summer of 2000, we made an addition that allows all of the system's channels to be switched from a high sensitivity mode, to a low sensitivity, so that we may more fully track a device's failure. The new components consist of a mezzanine card to be attached to each electrometer board, and an interface card and relay power supply card for each box. Each mezzanine card contains 4 Coto 9000 series ultra-low leakage current reed relays, Darlington drivers to switch the relays, and mounting points for the feedback resistors. Now instead of a single high value feedback resistor/ low leakage capacitor arrangement, we have a pair of feedback resistors (10G and 10M), which are connected in parallel using the reed relays, to switch from the high sensitivity mode, to low sensitivity. The mezzanine boards were designed in a horseshoe shape that piggybacks the existing electrometer card, while still allowing access to the AD549 electrometers for service and replacement. These mezzanine cards are controlled by the interface card, which in turn connects to the data acquisition system. This interface card also contains indicator LEDs to display the current channel and range. In addition we have now set all of the output buffers (OP-27) to a gain of 100, where before we had a mix of values dependent on the box number. Each box is now powered with +/- 24V and + 12V which is regulated locally to provide +/- 15V, +/- 12V, and +5V. The power and signals are connected to the boxes using ribbon cables.



The data acquisition computer, running Agilent (HP) Vee, controls the operation of the system. The current program is essentially a total rewrite of the original program, greatly increasing the modularity and encapsulation of the environment. Readability, and maintainability are also greatly improved. For the most part, operation of the system has remained unchanged. Data is still stored in a similar manner, with small changes in file structure to reflect data taken at different sensitivity ranges. The execution flow of the program is as follows:

- Check system constants file – rebuild if necessary
- Read existing sweep status file
- If last sweep has been completed, calculate resistances, and write data & summary files
- Create new sweep status file, reflecting the current step
- Change the bias level based on the current step
- Set the range relays to the high sensitivity
- Wait the appropriate period for the range setting
- Measure bias value at each box
- Measure leakage for n number of samples
- Write data to temp file
- Set the range relays to the low sensitivity
- Wait the appropriate period for the range setting
- Measure bias value at each box
- Measure leakage for n number of samples
- Write data to temp file
- Set the range relays to the high sensitivity
- Change the bias level based on the next step
- Compile leakage data into Jar Files
- Repeat steps 2-18 until user stops program

Using this procedure, we sweep all devices twice, once for each range. If a device is out of range on the high sensitivity mode, we throw out the data for that portion of the measurement.

To calibrate this system, it is now necessary to use two sets of calibration plugs, and to perform two separate sweeps. The calibration data is now stored separately from the jar data, and is merged by the device test program into a system constants file when the program is executed (Step 1 above). The calibration program compares the measured value of the calibration resistor against its known value, and computes a calibration constant that is now



associated with that channel. In this way each channel has two calibration constants, one for each range. The measurement program then uses this calibration constant to compensate the readings.

These modifications will allow greater measurement flexibility since all channels now allow testing through a wide range of resistance values, where before we had to hard wire a channel to read a specific narrow range. The modifications are complete except for final calibration and verification.

Passivation Chip

The pickup and decoder required further optimization to minimize noise and to maximize sensitivity. The decoder board mixes analog and digital circuitry, and must handle high speed pulse edges in order to accurately measure the time between pulses. The photo detector must transduce the photo signal to an electrical signal, and then detect the leading edge of the photo pulse accurately. This also requires high speed analog circuitry to optimize the measurement of the time interval between leading edges of the light pulses. These efforts are summarized below.

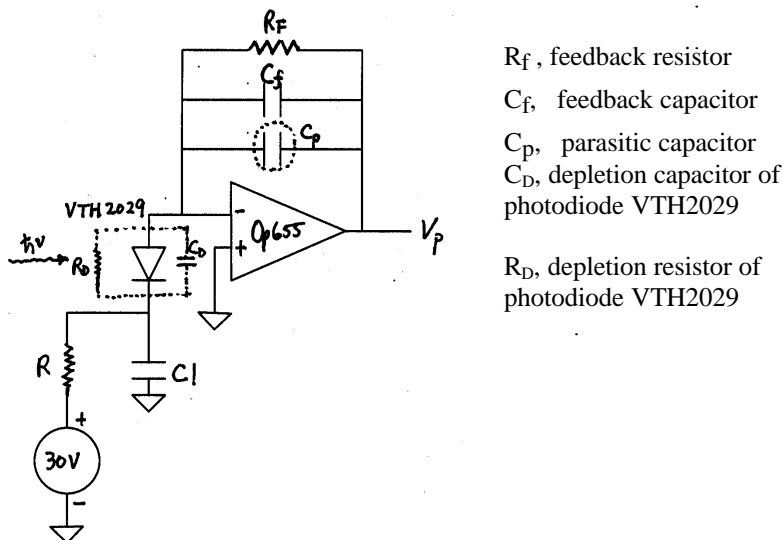


Figure 1. P030900 Pickup



Several studies have been conducted to optimize the slew rate and recovery time of the pickup, P030900 (Figure 1), and minimize the noise level at output of the threshold detectorII. ?

The experiment setup is shown in Figure 2. The LED and the pickup are mounted on two end sides of a 5x10x2 in. aluminum box. The LED is used as the light source to the pickup. The distance between the LED and photo detector of the pickup is 7 inches. The Al box is covered with a black cloth during the experiments to shield off interference from room lights. The frequency and intensity of the light pulse of the LED are controlled by Hp Function Generators 3311A & 3312A. Most experiments are conducted with a light source of 1uS pulse width and 10KHz frequency.

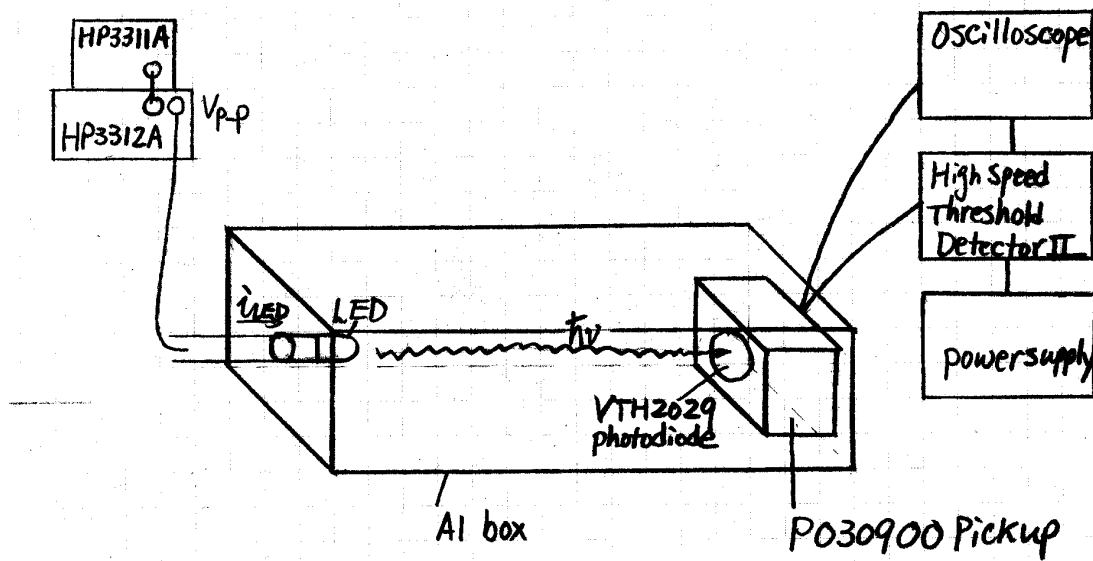


Figure 2. Experiment Setup

I) Feedback Resistor R_f ($C_f = 0$, $R = 0$, no 30V bias)

A set of R_f (247K Ω , 1M Ω , 10M Ω , 27M Ω) has been evaluated for their impact on slew rate (SR) and recovery time (τ) of the pickup as well as noise level of the threshold detector II output. The experimental results are shown in Tables 1, 2 & 3. We found that with a larger value of R_f , a faster slew rate and therefore an output with reduced noise can be achieved. However, the larger value of R_f will



also cause great delay of recovery time. As shown in Table1, an increase of R_f from $247K\Omega$ to $27M\Omega$ will delay recovery time from less than $1\mu S$ to $18\mu S$. These experiment results are consistent with the theory that the bigger feedback resistor results in a bigger close loop gain of OPA655. For the same light source (i_{LED}), a bigger close loop gain generates a bigger voltage output of OPA655 (V_p) and a sharper slew rate. On the other hand, $\tau = R_f C_{eq}$ where $C_{eq} = C_1 + C_p + C_f + C_D/A_v$ and A_v is the open loop gain of OPA655. τ is directly proportional to R_f ; bigger R_f , longer τ . A compromise between slew rate and τ has to be made. Since reduction of slew rate by an increase of R_f is less significant than the accompanying rise in recovery time, a smaller value of R_f should be used to achieve fast recovery time of the pickup. $R_f = 300 K\Omega$ will be chosen in the future design.

i_{LED} (mA)	τ ($R_f=247K\Omega$)	τ ($R_f=1M\Omega$)	τ ($R_f=10M\Omega$)	τ ($R_f=27M\Omega$)
11.1	540nS	1.24 μS	8 μS	18 μS
	Page 15	Page 7	Page 12	Page 13

Table 1. Recovery Time of Pickup (P030900) with $C_f=0$, $R=0$ and no 30V bias

i_{LED} (mA)	SR ($R_f=247K\Omega$) mV/ μS	SR ($R_f=1M\Omega$) mV/ μS	SR ($R_f=10M\Omega$) mV/ μS	SR ($R_f=27M\Omega$) mV/ μS
0.44			37	34
0.77		51	69	71
0.93	49			
1.54	88	122	167	160
4	265	413	519	510
6	400	653	789	757
8	546	867	973	1070
10	688	1030	1260	1360
11.1	747	1150	1360	1450
	Page 15	Page 7	Page 12	Page 11

Table 2. Slew Rate of Pickup (P030900) with $C_f=0$, $R=0$ and no 30V bias

i_{LED} (mA)	Noise ($R_f=247K\Omega$) nS	Noise ($R_f=1M\Omega$) nS	Noise ($R_f=10M\Omega$) nS	Noise ($R_f=27M\Omega$) nS
0.44			675	720
0.77		390	265	270



0.83				
0.93	390			
1.54	155	152	120	120
4	72	50	40	40
6	40	32	28	28
8	32	24	23	24
10	26	23	16	16
11.1	24	16	16	16
	Page 15	Page 7	Page 12	Page 11

Table 3. Noise of Threshold Detector II Output with $C_f=0$, $R=0$ and no 30V biasII) Capacitor C1 ($R_f=10\text{ M}\Omega$, $C_f=0$, $R=0$, no 30V bias)

A capacitor C1 is necessary to block low frequency noises such as 60Hz cycles found in room lights. However, a bigger value of C1 will impose a smaller impedance ($Z \propto 1/\omega C$). Therefore more light signals can be detected by the photo detector which results in a faster slew rate. Moreover, experiments shows that a large C1 is necessary in order to shield off electrical interference. The effect of C1 on slew rate and electrical interference is exhibited in the following experiment. With a fixed light source, photo detector VTH2090 is initially placed 7 inches from the LED to measure the slew rate (Figure 2) and then placed directly against the LED with a black tape between (Figure 3) to measure any output V_p from the photo detector (electrical interference). A set of C1 (1pF, 11pF, 111pF, 1000pF, 10000pF, ∞) is evaluated and the results are shown in Table 4 and Figure 4. We found that slew rate is indeed proportional to C1 and at $C1=10,000\text{pF}$, electrical interference is negligible and 60Hz noise is not observed. $C1=10,000\text{pF}$ will be used.

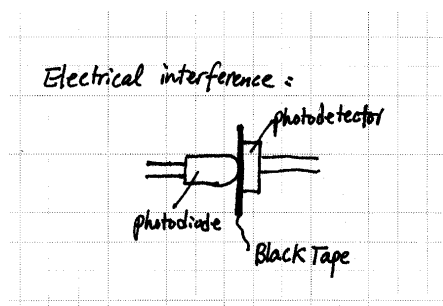


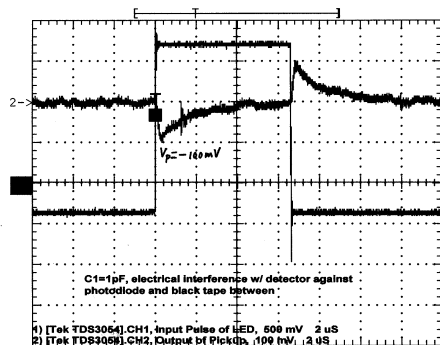
Figure 3. Setup for electrical interference study



C1 (pF)	V _p (mV)	SR (V/μS)
1	-100	0.037
11	-80	0.108
111		0.64
1000	-28	1.19
10000	-15	1.38
	negligible	4.52

Table 4Electrical interference, V_p and Slew Rate (SR) vs. C1

Datasheet: YTSheet (5) Page: 1



Datasheet: YTSheet (9) Page: 1

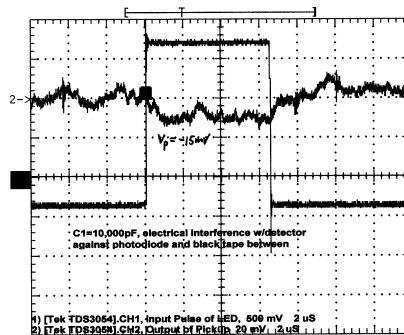


Figure 4. Electrical Interference artifact at C1=1pF and C1=10,000pF

**III) 30V bias with $R_f = 300 \text{ K}\Omega$ and $R = 1 \text{ M}\Omega$**

To improve slew rate and recovery time of the pickup, it is very important to minimize depletion capacitance of the photodiode VTH2029, C_D . A 30V bias has been directly applied onto VTH2029 to increase the depletion region of the photodiode, therefore reducing C_D . The impressive results of 30V bias effects are shown in Table 5.

	no bias, $C_f = 0 \text{ pF}$ output load = 500Ω	30V bias, $C_f = 0.25 \text{ pF}$ output load = 500Ω	30V bias, $C_f = 0.25 \text{ pF}$ output load = 100Ω
$i_{LED}(\text{mA})$	SR(V/uS)	SR(V/uS)	SR(V/uS)
0.53			0.099
0.564		0.122	
0.64	0.052		
8	1.02	2.8	2.33
11	1.33	3.82	3.19
$i_{LED}(\text{mA})$	Noise (nS)	Noise (nS)	Noise (nS)
0.53			150
0.564		150	
0.64	320		
8	16	5.6	5
11	12	3.6	3.6
$i_{LED}(\text{mA})$	τ (nS)	τ (nS)	τ (nS)
11	648	188	240
	YT sheet(22)	YT sheet(24)	YT sheet(26)

Table 5. 30V bias effect on slew rate, noise, and recovery time τ

By applying 30V bias, slew rate, noise and recovery time τ all have been improved about three times as compared with the results with no bias.

IV) Feedback Capacitor C_f , Resistor R , Output load

It was found that with 30V bias applied, a small feedback capacitor C_f is sometimes necessary to avoid ringing at pickup output. The effect of C_f is shown



in Figure 5 and the value of C_f depends on intrinsic nature of the circuits, parasitic capacitance C_p . In our protocol study (P030900), a value of 0.25pF is necessary to avoid output ringing, however no C_f is needed in the final printed circuits (PT052100). The comparison of P030900 and PT052100 is shown in Table 6.

The bias voltage current limiting resistor R effects circuit performance by shunting photodiode current if it has a lower impedance than the effective input impedance of the amplifier. A set of R ($R=10k\Omega$, $100k\Omega$, $500k\Omega$, $1M\Omega$) was evaluated. It was found that $R > 100k$ had no obvious effect on the pickup performance as shown in Figure 6.

A final set of experiments was conducted to evaluate influence of output load of the pickup on its output V_p . It was found that reducing output load will dampen the rings and reduce the noise at rising edge of V_p as shown in Figure 7, therefore giving cleaner shutoff at threshold detector output V_{out} . Although reducing output load of the pickup will slightly slow the slew rate and delay its recovery time, this negative impact is very limited as indicated in Table 5. Comparing pro and con, a low output load of pickup (100Ω) was used in the final design to achieve a cleaner shutoff of V_{out} .

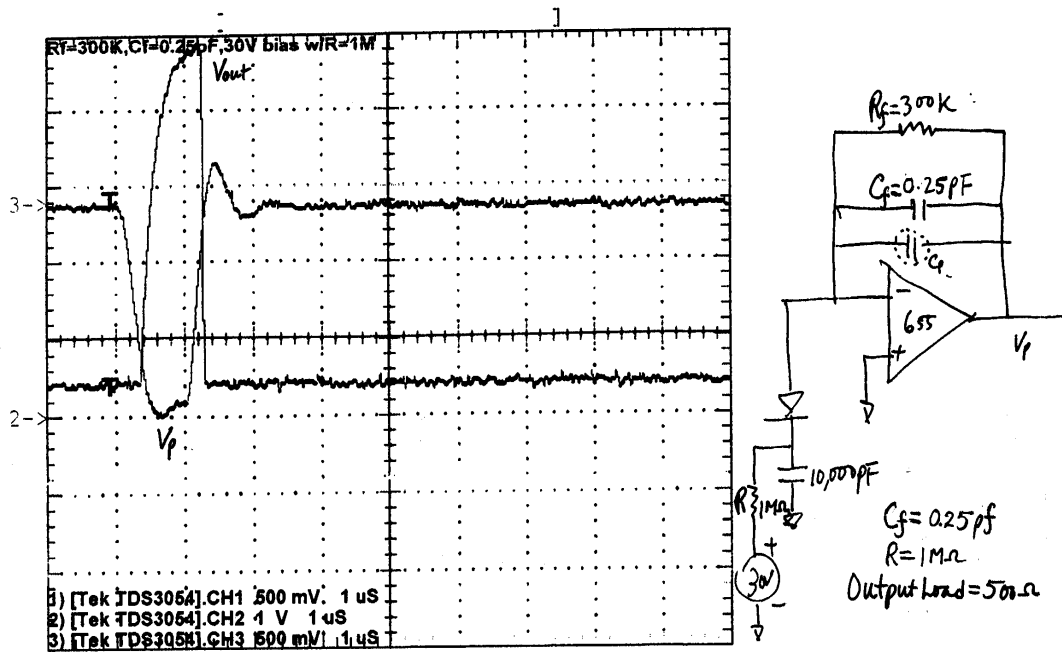
	P030900	PT052100
	$R_f=300K, C_f=0.25pF, 30V$ bias	$R_f=332K$, no C_f , 30V bias
	output load= 100Ω , $i_{LED}=11mA$	output load= 100Ω , $i_{LED}=16mA$
SR (V/uS)	3.19	4.3
Noise (nS)	3.6	1.6
τ (nS)	240	240

Table 6. Comparing prototype P030900 and final version PT052100





Datasheet: YTSheet (24) Page: 1



Datasheet: YTSheet (21) Page: 1

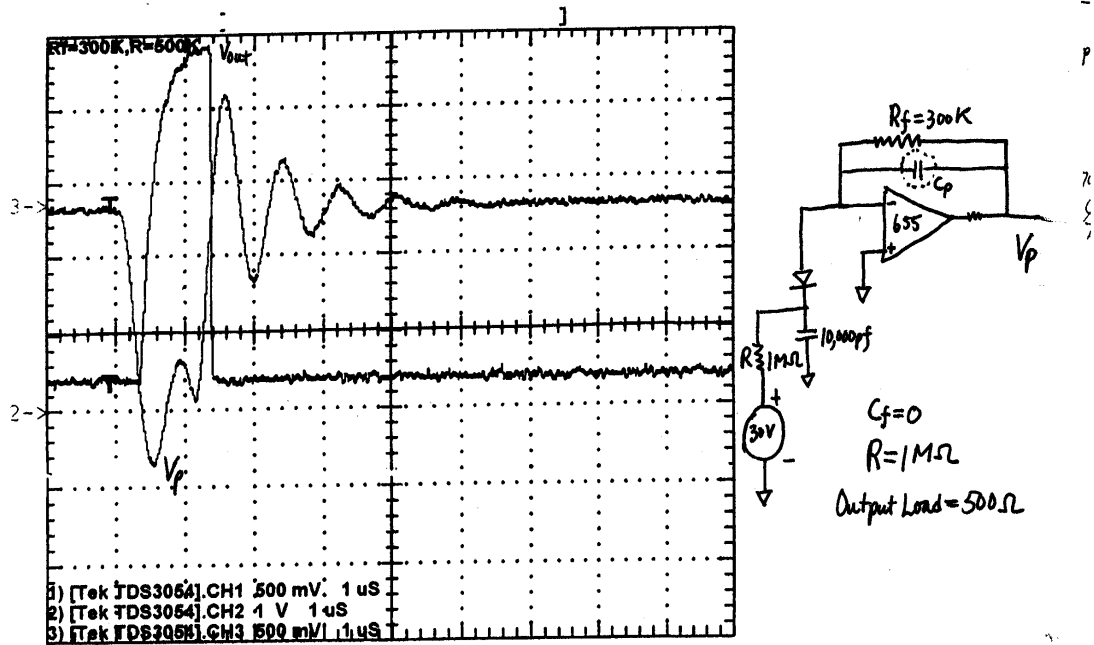
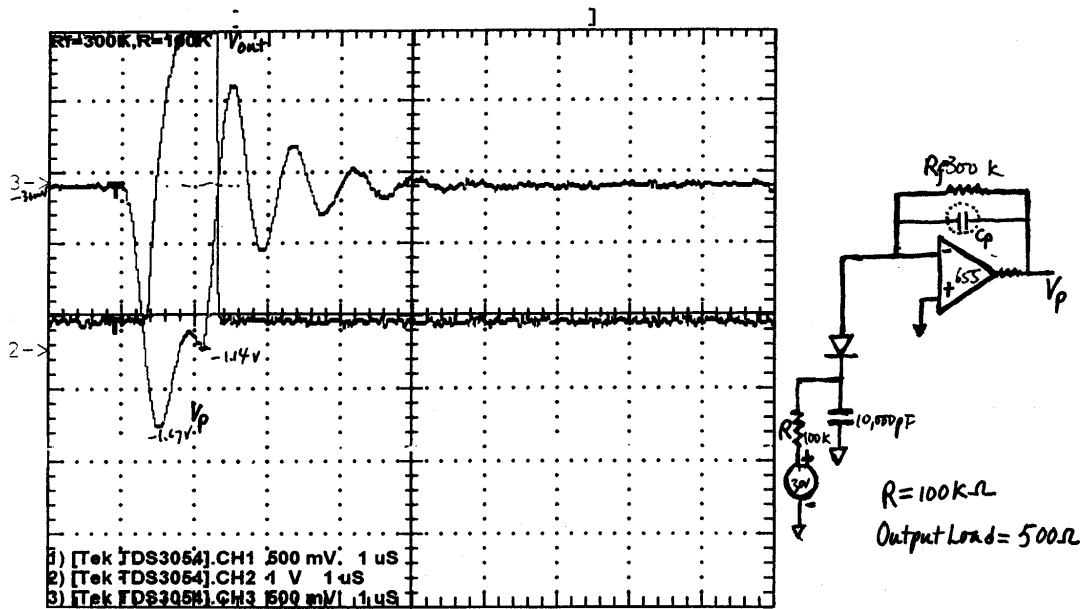


Figure 5. Effect of C_f on pickup output ringing



Datasheet: YTSheet (19) Page: 1



Datasheet: YTSheet (21) Page: 1

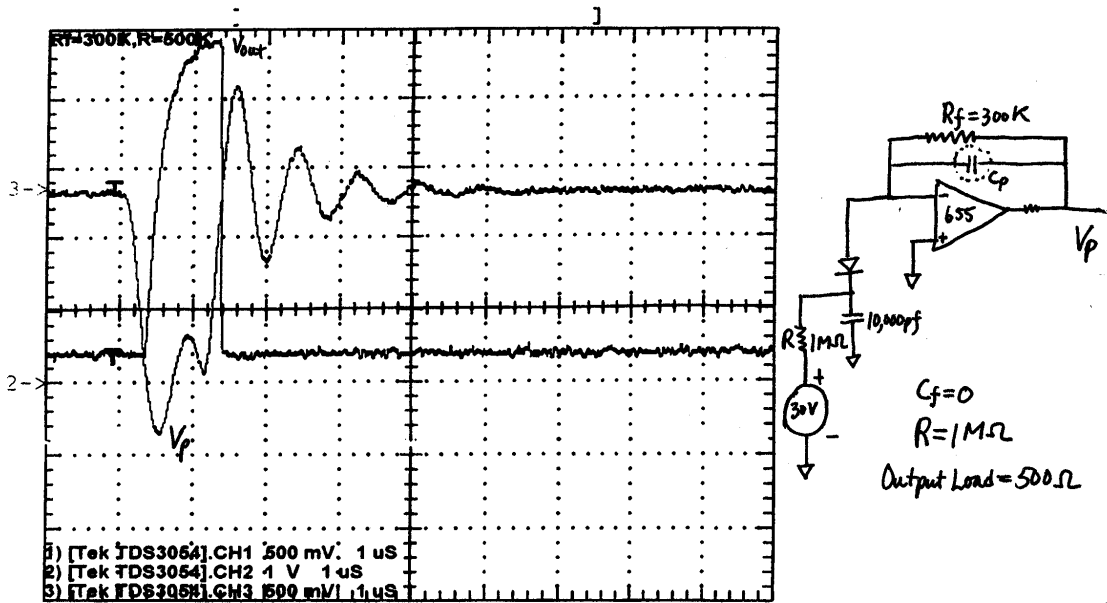
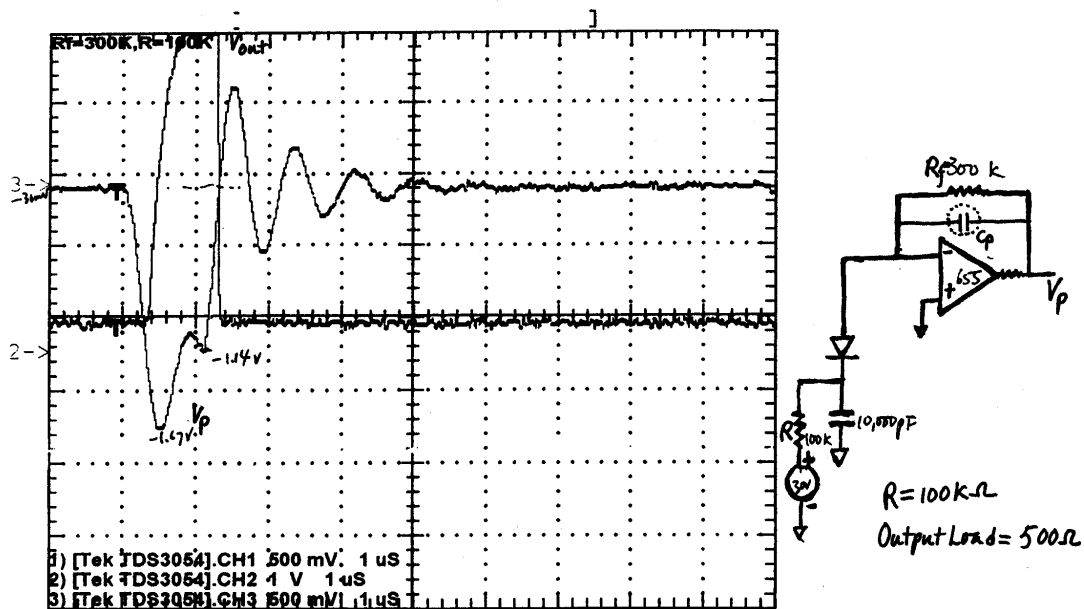


Figure 6. Pickup Output V_p (P030900) with $R=100 K\Omega$ and $1M\Omega$



Datasheet: YTSheet(19) Page: 1



Datasheet: YTSheet(20) Page: 1

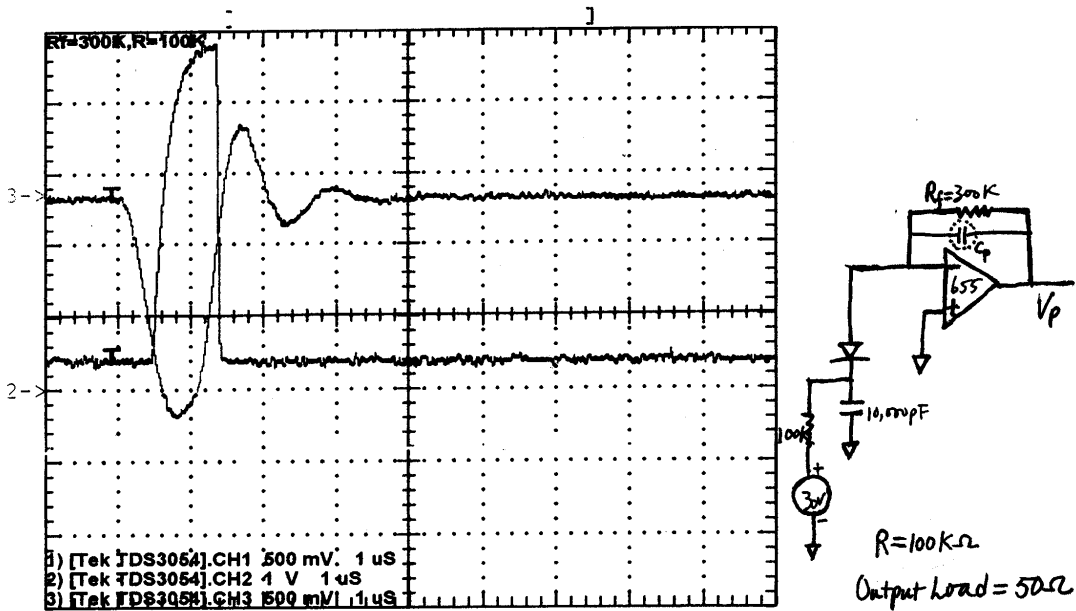


Figure 7. Pickup Output V_p with output load= 500Ω and 50Ω



Interdigitated Electrode Arrays for Evaluation of Intra-Cortical Insulators

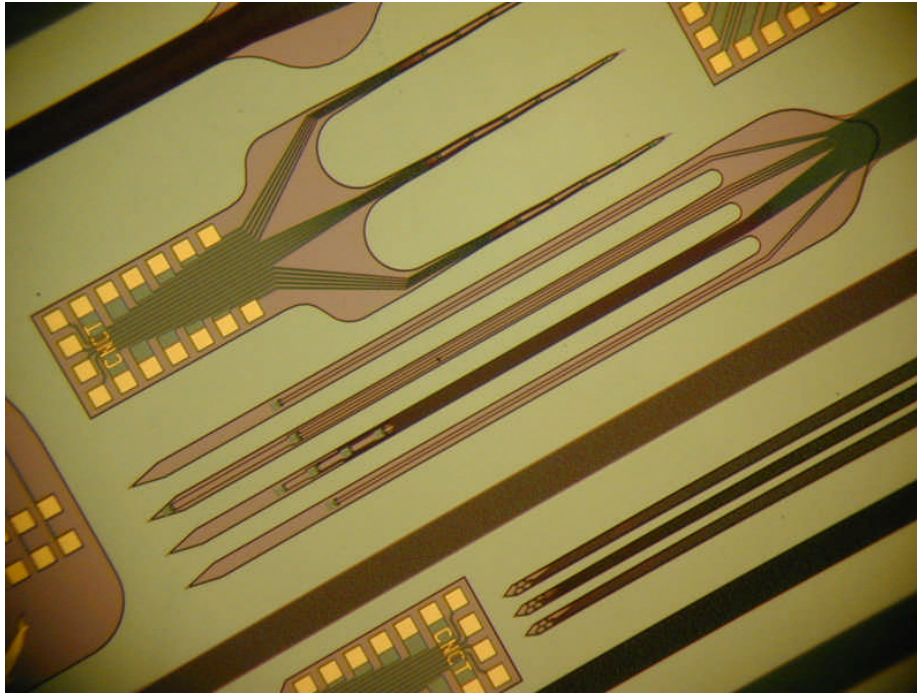


Figure 8: Microphotograph of IDE array on silicon microprobe fabricated by UM. Photo complements of J. Hetke.

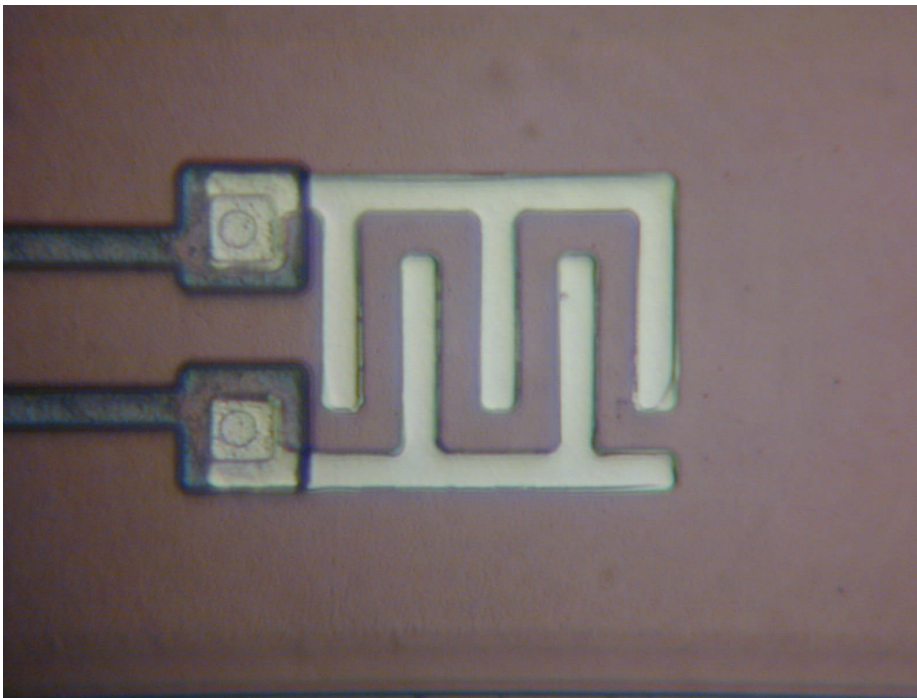


Figure 9: Close up of 3um spaces and traces of IDE and polysilicon contacts fabricated by UM. Photo complements of J. Hetke.



Interdigitated Electrode Arrays (IDEs) on silicon microprobes were fabricated by the University of Michigan Center for Neural Communication Technology. A microphotograph of one of the arrays still on the wafer is shown in Figure 8. Four IDEs were located in a column at 200 μ m intervals along one of the center shafts with the closest approximately 500 μ m away from the tip. These will be used to check for local surface conductivity, local variations along the shaft, and far reaching surface conductive pathways along the shaft separated by 200 μ m, 400 μ m, or 600 μ m (by pairing half of 2 IDEs). Three additional IDEs will be located adjacent to a central IDE to form a row of 4 (with one on each shaft) approximately 700 μ m away from the tips. This row will be used to check for variations in local surface conductivity due to shaft location during coating (in a plasma for instance), and to quantify bulk material characteristics independent of surface leakage properties. Since there were 2 bonding pins leftover, an IDE was located at the tip of one shaft to allow evaluation of shaft tip effects. 3 μ m traces and spaces were used to form the IDEs in iridium as shown in Figure 9. Devices will be tested for functionality next quarter.